THE JOURNAL OF BIOLOGICAL CHEMISTRY VOL. 287, NO. 28, pp. 23852–23863, July 6, 2012

Perilipin 5, a Lipid Droplet-binding Protein, Protects Heart from Oxidative Burden by Sequestering Fatty Acid from Excessive Oxidation*◆

Received for publication, November 29, 2011, and in revised form, April 13, 2012 Published, JBC Papers in Press, April 24, 2012, DOI 10.1074/jbc.M111.328708

Kenta Kuramoto[‡1], Tomoo Okamura[‡1], Tomohiro Yamaguchi[‡§1], Tomoe Y. Nakamura[¶], Shigeo Wakabayashi[¶], Hidetaka Morinaga[‖], Masatoshi Nomura[‖], Toshihiko Yanase[‖], Kinya Otsu[**], Nobuteru Usuda[‡‡], Shigenobu Matsumura[§§], Kazuo Inoue[§§], Tohru Fushiki[§§], Yumiko Kojima[‡], Takeshi Hashimoto[‡2], Fumie Sakai[‡], Fumiko Hirose[‡], and Takashi Osumi[‡3]

From the [‡]Graduate School of Life Science, University of Hyogo, Kamigori, Hyogo 678-1297, Japan, the [§]School of Pharmaceutical Sciences, Showa University, Tokyo 142-8555, Japan, the [¶]Department of Molecular Physiology, National Cerebral and Cardiovascular Center Research Institute, Suita 565-8565, Japan, the [‖]Department of Medicine and Bioregulatory Science, Kyushu University, Fukuoka 812-8582, Japan, the [**]Cardiovascular Division, King's College London, London SE5 9NU, United Kingdom, the [‡‡]Department of Anatomy II and Cell Biology, Fujita Health University School of Medicine, Toyoake, Aichi 470-1192, Japan, and the [§§]Division of Food Science and Biotechnology, Graduate School of Agriculture, Kyoto University, Kyoto 606-8502, Japan

Background: Perilipin family proteins are important in determining the properties of lipid droplets (LDs).
Results: Perilipin 5-deficient mice lack detectable LDs, exhibit enhanced fatty acid oxidation, and suffer increased ROS production in the heart.
Conclusion: Perilipin 5 protects the heart from oxidative burden by sequestering fatty acid from excessive oxidation.
Significance: These findings may help to increase understanding of the functions of non-adipose LDs.

Lipid droplets (LDs) are ubiquitous organelles storing neutral lipids, including triacylglycerol (TAG) and cholesterol ester. The properties of LDs vary greatly among tissues, and LD-binding proteins, the perilipin family in particular, play critical roles in determining such diversity. Overaccumulation of TAG in LDs of non-adipose tissues may cause lipotoxicity, leading to diseases such as diabetes and cardiomyopathy. However, the physiological significance of non-adipose LDs in a normal state is poorly understood. To address this issue, we generated and characterized mice deficient in perilipin 5 (Plin5), a member of the perilipin family particularly abundant in the heart. The mutant mice lacked detectable LDs, containing significantly less TAG in the heart. Particulate structures containing another LD-binding protein, Plin2, but negative for lipid staining, remained in mutant mice hearts. LDs were recovered by perfusing the heart with an inhibitor of lipase. Cultured cardiomyocytes from *Plin5*-null mice more actively oxidized fatty acid than those of wild-type mice. Production of reactive oxygen species was increased in the mutant mice hearts, leading to a greater decline in heart function with age. This was, however, reduced by the administration of *N*-acetylcysteine, a precursor of an antioxidant, glutathione. Thus, we conclude that Plin5 is essential for maintaining LDs at detectable sizes in the heart, by antagonizing lipase(s). LDs in turn prevent excess reactive oxygen species production by sequestering fatty acid from oxidation and hence suppress oxidative burden to the heart.

Lipid droplets (LDs)[4] are cellular organelles storing neutral lipids, including triacylglycerol (TAG) and cholesterol ester. LDs are found in nearly all cell types, but their properties vary greatly among tissues. White adipose tissue (WAT) has large unilocular LDs that store an enormous amount of TAG in case of increased energy demand. LDs of other tissues, however, are usually much smaller. Their physiological significance is less well understood, although a possible role is in sequestering fatty acid (FA) in a chemically inert form, TAG, to circumvent the lipotoxicity of FA and its derivatives (1). However, excess accumulation of TAG, and hence aberrant development of LDs, often causes lipotoxicity, leading to diseases such as diabetes and cardiomyopathy.

LDs carry a defined set of surface-binding proteins whose compositions differ among cell types. The perilipin family, conventionally called the PAT family, is a representative group of LD-binding proteins composed of five members (2). The recently proposed unified nomenclature (3) names them PLIN1 (the classic perilipin), PLIN2 (also named ADRP, ADFP, or adipophilin), PLIN3 (Tip47, PP17, or M6PRBP), PLIN4 (S3–12),

* This work was supported in part by grants-in-aid for scientific research from the Japan Society for the Promotion of Science (to T. O.) and for Young Scientists (to T. Y.) and by the Global Center of Excellence Program (Pico-biology, Life Science at the Atomic Level), Ministry of Education, Culture, Sports, Science, and Technology, Japan.
◆ This article was selected as a Paper of the Week.
[1] These authors contributed equally to this work.
[2] Present address: Faculty of Sport and Health Science, Ritsumeikan University, Kusatsu, Shiga 525-8577, Japan.
[3] To whom correspondence should be addressed. Tel.: 81-791-58-0192; Fax: 81-791-58-0193; E-mail: osumi@sci.u-hyogo.ac.jp.

[4] The abbreviations used are: LD, lipid droplet; TAG, triacylglycerol; WAT, white adipose tissue; FA, fatty acid; BAT, brown adipose tissue; ATGL, adipose triacylglycerol lipase; HSL, hormone-sensitive lipase; ROS, reactive oxygen species; NAC, *N*-acetylcysteine; ORO, Oil Red O; BEL bromoenol lactone; TBARS, thiobarbituric acid-reactive substance; LVID;d, left ventricular end-diastolic dimension; LVID;s, left ventricular end-systolic dimension; FS, left ventricular fractional shortening; ASM, acid-soluble material.

and PLIN5 (MLDP, OXPAT, LSDP5, or PAT1). These proteins have related amino acid sequences, particularly in the amino-terminal region called the PAT1 domain (2). Plin1 (the mouse homolog of human PLIN1) is highly abundant in WAT and brown adipose tissue (BAT). Plin2 and Plin3 are expressed in many cell types, whereas Plin4 is abundant in adipose tissue. In contrast, we (4) showed that Plin5 is highly concentrated in the heart, whereas other groups (5, 6) demonstrated that this protein is expressed in oxidative tissues, including the heart, BAT, skeletal muscle, and the liver.

Plin1 is the best characterized member of the perilipin family, playing a central function in both the storage and catecholamine-dependent mobilization of TAG in WAT (7, 8). Recent studies (9–15) have presented an elaborate model for the actions of Plin1 involving adipose triacylglycerol lipase (ATGL), comparative gene identification (CGI)-58 (also called α,β-hydrolase domain-containing 5), a coactivator of ATGL, and hormone-sensitive lipase (HSL) (for review see Ref. 16). The functions of other perilipin family members are less well understood, although the proteins were shown to protect TAG from attack by lipases (17). *Plin2*$^{-/-}$ mice are resistant to a high fat diet-induced hepatosteatosis (18), and Plin3 compensates for the defect of Plin2 in these mice (19).

Some 60–70% of the large energy demand of the heart for contractile function is fulfilled by FA (20). Thus, the heart has an extremely high capacity of lipid turnover and particularly small LDs. We presumed that Plin5 has a critical role in determining the properties and functions of LDs in the heart, and hence it is the key to understanding the physiological significance of heart LDs. Accordingly, we generated and characterized *Plin5* knock-out (*Plin5*$^{-/-}$) mice. To our surprise, *Plin5*$^{-/-}$ mice lacked detectable LDs in the heart, substantiating the essential role of Plin5 in maintaining heart LDs. These mice suffered from an accelerated decline in heart contractile function with age, probably due to increased production of reactive oxygen species (ROS). We propose that LDs contribute to suppressing oxidative stress in the heart by sequestering FA from excessive oxidative metabolism.

EXPERIMENTAL PROCEDURES

Mice—Plin5$^{-/-}$ mice were produced by using the standard gene disruption procedure (Fig. 1*A*). The *Plin5*$^{-/-}$ mice were backcrossed to the C57BL/6J strain (CLEA Japan, Inc.) for four generations. *Plin5*$^{+/+}$ and *Plin5*$^{-/-}$ mice were obtained by mating respective homozygous parents. Mice were housed under standard conditions at 24–26 °C with a 12:12 h light/dark cycle and given free access to standard chow (CLEA Japan, Inc.) and water. For some experiments, mice were fasted overnight by food deprivation. For the treatment with *N*-acetylcysteine (NAC), the chemical was dissolved in water at 1.88 mg/ml and given to the mice instead of water. The treatment was continued from 16 to 18 weeks of age to the day of experiment at 30–32 weeks of age, replacing the solution every 2–3 days. Assuming that mice 30 g in body weight drink 8 ml of water per day on average (21), this dose would correspond to 500 mg of NAC/kg/day. All procedures were performed in accordance with the guidelines established by University of Hyogo for the care and use of experimental animals.

Histological Analyses—Tissues were fixed with 10% formalin/PBS, incubated with 10% sucrose/PBS, and then with 20% sucrose/PBS, each overnight at 4 °C. The tissues were embedded in O.C.T. compound (Tissue-Tek) and sectioned 10 μm thick in a cryostat (Leica CM3050S-III). Sections were air-dried and stored at −80 °C until used. After removal of the O.C.T. compound by washing with water, sections were stained for lipid with 0.18% Oil Red O (ORO) in 60% isopropyl alcohol. Sections were washed with 60% isopropyl alcohol, counterstained with hematoxylin, and subjected to microscopic analysis.

Immunofluorescence Staining—Cryosections as prepared above were freed from the O.C.T. compound and permeabilized with methanol for 20 min at −20 °C. After washing with PBS three times for 5 min each at room temperature, sections were blocked with 2% BSA/PBS for 1 h at room temperature. Sections were then incubated with primary antibodies to Plin5 (raised in rabbit (4)) and Plin2 (raised in guinea pig) and diluted 1000-fold in 2% BSA/PBS overnight at 4 °C. Secondary antibodies, Alexa 488- and 594-conjugated anti-guinea pig and rabbit IgG (Molecular Probes), respectively, were used at a 500-fold dilution in 2% BSA/PBS for 1 h at room temperature. For double staining of Plin5 and lipid, permeabilization with methanol was omitted to avoid a loss of lipid. Because of freezing and thawing of the cryosections, antibodies were allowed to access intracellular compartments, although the fluorescence signals were inevitably weaker than those obtained by usual permeabilization. Sections were first stained for Plin5 and then with 100 μM Bodipy 493/503 (Molecular Probes). Samples were examined in a confocal laser microscope (Zeiss LSM510).

Electron Microscopy—Dissected tissues were prefixed with 2% glutaraldehyde/PBS at 4 °C. After being washed with PBS, tissues were fixed with 2% osmium tetroxide/PBS for 2 h at 4 °C. Specimens were embedded in Quetol-812 (Nissin EM), and then sectioned and observed in a JEM-1200EX (JEOL).

Biochemical Analyses—Lipids were extracted from tissues according to a standard procedure (22). TAG and FA levels were measured using triglyceride *E*-test (WAKO) and nonesterified fatty acid *C*-test (WAKO), respectively. Protein was determined with a protein assay kit (Bio-Rad), using BSA as a standard.

Immunoblot Analysis—Protein extracts were prepared from tissues by using lysis buffer (20 mM Tris-HCl (pH 7.5), 1% Triton X-100, 150 mM NaCl, 10 mM NaF, 1 mM sodium pyrophosphate, 1 mM sodium orthovanadate, protease inhibitor mixture (Roche Applied Science), and 1 mM EDTA). Protein concentrations were quantified, and the extracts were subjected to immunoblotting.

RT-PCR—Total RNA was prepared from cardiac ventricles using QIAzol reagent (Qiagen) and reverse-transcribed. Target genes were amplified with a SYBR qPCR kit (KAPA Biosystems) and quantified using an ABI PRISM7000 (Applied Biosystems).

Subcellular Fractionation—The hearts from fed and fasted wild-type and *Plin5*$^{-/-}$ mice were homogenized in 500 μl of 20 mM Hepes-NaOH (pH 7.4) containing protease inhibitor mixture (Roche Applied Science), using a Potter-Elvehjem homogenizer. After the removal of nuclei and cell debris by centrifugation at 700 × *g* for 10 min, 300 μl of the postnuclear

supernatant was mixed with an equal volume of 60% sucrose and placed below a 5-ml 0–30% (w/v) sucrose gradient in a centrifuge tube. Samples were centrifuged for 6 h at a maximal gravity of 140,000 × *g* at 4 °C in a swinging bucket rotor, S52ST, in a Hitachi CS100GXL ultracentrifuge. Samples were collected into 24 consecutive portions of 230 μl each from the top and combined into eight fractions by mixing three consecutive portions for subsequent analyses. Because a substantial amount of pellet was obtained at the bottom, it was resuspended in 230 μl of 30% sucrose, 10 mM Hepes-NaOH (pH 7.4), and numbered as fraction 9. For immunoblotting, a one-third volume of fraction 9 relative to those of fractions 1–8 was loaded onto gels. In another centrifugal experiment, 0–51.2% (w/v) sucrose gradient was employed.

Inhibition of ATGL and Related Lipases in the Heart—Mice fasted overnight were perfused with 10 ml of 50 μM bromoenol lactone (BEL) in saline for 6 min. The heart was then immediately isolated and analyzed. For the visualization of LDs, Nile Red staining was performed with frozen sections. *In vitro* lipase assay was performed as described (23).

Isolation of Cardiomyocytes—Ventricular myocytes were obtained as described previously (24). Briefly, ventricular tissues isolated 1.5–3 days after birth were cut into small pieces and digested to produce single cells with an enzyme solution (3:1 mixture of 1 mg/ml collagenase and 0.25% trypsin in PBS). The cells obtained were seeded into collagen-coated 35-mm dishes and incubated in 2 ml of Dulbecco's modified Eagle's medium (DMEM), 10% fetal bovine serum. After incubation overnight, attached cells were subjected to an FA oxidation assay.

FA Oxidation Assay—In each experiment, cardiomyocytes obtained from 3 to 4 mice were seeded into six 35-mm dishes and incubated overnight, as described above. Cells were cultured for a further 2 days in DMEM, 10% fetal bovine serum supplemented with 200 μM oleic acid conjugated with BSA to allow most cells to start spontaneous beating. Cells were then treated with 1 ml of preincubation medium (DMEM, 200 μM oleic acid) with or without 40 μM etomoxir (three dishes each) for 1 h. Subsequently, cells were incubated in 1 ml of the assay medium (DMEM, 20 mM Hepes-NaOH (pH 7.4) containing 4 μM [1-^{14}C]palmitic acid conjugated with α-cyclodextrin), supplemented with or without 40 μM etomoxir for 1 h. During this procedure, each 35-mm dish was uncovered and put in a covered 10-cm dish containing a piece of filter paper soaked in 1 N NaOH to trap radioactive CO_2 ("1st filter paper"). After incubation, the culture supernatants were transferred to test tubes, and the cells were dissolved in 300 μl of cell lysis buffer (25 mM Tris-HCl (pH 7.5), 1 mM EDTA, 0.1% Triton X-100). Protein concentrations of the cell lysates were quantified for 50-μl aliquots. One hundred microliters of 10% BSA followed by 150 μl of 3 M perchloric acid were added to the remaining cell lysates, which were then mixed and centrifuged. The supernatants contained intracellular acid-soluble materials (ASM), representing active metabolic intermediates. The pellet was extracted with chloroform/methanol (2:1), and the organic layer was collected (intracellular acid-insoluble fraction, representing cellular lipids). The culture supernatants were also mixed with BSA and perchloric acid and left for 30 min at room temperature, during which time the tubes were covered with parafilm attached with NaOH-soaked filter paper to trap CO_2 forced out from the culture supernatants ("2nd filter paper"). The mixtures were then centrifuged and separated into acid-soluble (extracellular ASM, representing dead-end metabolites such as acetic acid) and acid-insoluble (extracellular acid-insoluble fraction, mostly representing unincorporated FA) fractions, as described above. The filter paper and soluble and insoluble fractions were subjected to scintillation counting. β-Oxidation activity was assessed by the radioactivity of CO_2 (sum of radioactivities of 1st and 2nd filter papers), intracellular as well as extracellular ASM, with the first two representing metabolites en route to complete oxidation in mitochondria. Incorporation of FA was evaluated from the sum of the radioactivity of CO_2, intracellular and extracellular ASM, and the intracellular acid-insoluble fraction. Values obtained for three culture dishes were averaged and used as a result of a single experiment.

Measurements of Blood Parameters—Blood glucose levels were determined by Glutest sensor (SKK). Serum ketone bodies were determined with a β-hydroxybutyrate assay kit (Cayman). Insulin was quantified using an insulin ELISA kit (Shibayagi).

Food Intake, Respiration, and Locomotion—Mice were put in cages individually and allowed to access food and water *ad libitum* during the experiment. Food intake was measured for 10 days, and average intake per day was calculated. The respiratory gas analysis was performed with an Arco-2000 (Arco System), as described previously (25). Locomotor activity was measured with a 14-channel DAS system (Neuroscience).

Thiobarbituric Acid-reactive Substance (TBARS) Assay—Heart tissue samples were homogenized in lysis buffer as described above. Protein concentrations were quantified, and the extracts were subjected to a TBARS analysis, according to a published procedure (26), with slight modifications.

Echocardiography—For age-matched mice under 1.5% isoflurane anesthesia, heart rate and rhythm were monitored using 4-limb-lead electrocardiography (TMH150, Visual Sonics). Left ventricular contractile forces were quantified by transthoracic echocardiography using Vevo2100 (Visual Sonics). The percentage of left ventricular fractional shortening (FS) was calculated as follows: ((LVID;d − LVID;s)/LVID;d) × 100, where LVID;d and LVID;s indicate left ventricular end-diastolic and end-systolic dimensions, respectively. When the animals were also subjected to a TBARS assay, the hearts were excised several days after the echocardiographic measurement.

Statistical Analysis—All data are shown as means ± S.E. Data were analyzed with Student's *t* test, and differences with $p < 0.05$ were considered statistically significant. The correlation between heart parameters and TBARS values was assessed by a regression analysis.

RESULTS

Generation of Plin5-deficient Mice—*Plin5*$^{-/-}$ mice were generated (Fig. 1, *A* and *B*), and the absence of Plin5 mRNA and protein in tissues of mutant mice was confirmed (Fig. 1, *C* and *D*). Expression of *Plin4*, a close neighbor of *Plin5* in the genome, was not affected (Fig. 1*C*). Intercrossing of *Plin5*$^{+/-}$ mice provided *Plin5*$^{-/-}$ offspring at a Mendelian ratio. Deletion of *Plin5* caused no abnormality in either cumulative body weight or

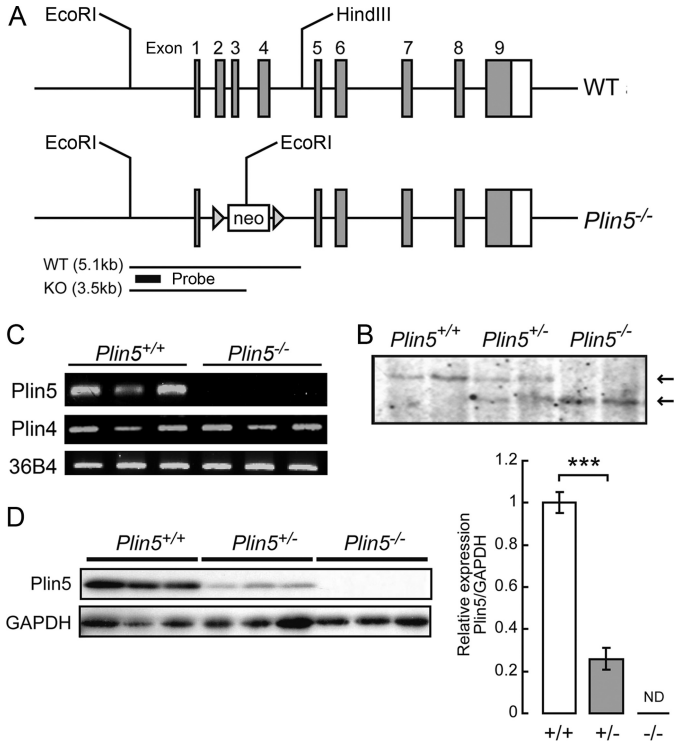

FIGURE 1. **Generation of Plin5 knock-out mice.** *A,* structures of wild-type and null Plin5 alleles. *B,* confirmation of *Plin5* disruption by Southern blotting with genomic DNA prepared from the tail. *Arrows* indicate wild-type (*WT*) and knock-out (*KO*) bands corresponding to the fragments depicted in *A*. *C,* RT-PCR to reveal the absence of Plin5 mRNA in the hearts of *Plin5*$^{-/-}$ mice. Plin4 mRNA was expressed at the normal level. *D,* confirmation of the absence of Plin5 protein in the hearts of *Plin5*$^{-/-}$ mice. The *graph* on the *right* shows the Plin5/GAPDH ratios of mice of the three genotypes. *ND*, not detectable; ***, $p < 0.001$.

body length (data not shown). Weights of tissues, including the heart, were not significantly different between the two genotypes of mice at 16–20 weeks of age (data not shown). Thus, *Plin5* deficiency does not cause apparent defects in growth and development. Further experiments were performed with male mice of age 16–20 weeks, unless otherwise noted.

Absence of LDs in the Hearts of Plin5$^{-/-}$ *Mice*—Based on the particularly abundant expression of Plin5 in the heart (4), we expected its deficiency to affect the properties of LDs most prominently in the heart. Accordingly, we first stained the heart sections of wild-type and *Plin5*$^{-/-}$ mice with ORO (Fig. 2*A*). In wild-type mice, small LDs were observed in a limited number of heart cells in the fed state. LDs were markedly augmented upon fasting as reported previously (27), due to increased delivery of FA from WAT. Surprisingly, no LDs were detected in the hearts of *Plin5*$^{-/-}$ mice by ORO staining either in the fed or fasted state. By electron microscopy, LDs were not observed in the hearts of fasted *Plin5*$^{-/-}$ mice (Fig. 2*B*). We also measured the content of TAG and FA in the heart. Consistent with the apparent absence of LDs, the TAG content in the hearts of *Plin5*$^{-/-}$ mice was lower than that in control mice (Fig. 3*A, panel a*), in both fed and fasted animals. The FA level was also lower in the hearts of *Plin5*$^{-/-}$ mice than that of wild-type mice (Fig. 3*B, panel a*).

Lipid and LD Contents of Other Tissues—Effect of Plin5 ablation on the contents of TAG and FA was also examined for other tissues. In soleus muscle, TAG content tended to be slightly lower in *Plin5*$^{-/-}$ mice than in control mice in the fed state, but it was not significantly different between them in the fasted state (Fig. 3*A, panel b*). FA content was not significantly different either between the two genotypes, although it was severely reduced by fasting (Fig. 3*B, panel b*). Upon ORO staining, LDs were detected in a small number of myotubes in both genotypes, when the mice were fasted (Fig. 2*C*). Their size and abundance were slightly greater in the wild-type mice. In the liver, levels of both TAG (Fig. 3*A, panel c*) and FA (Fig. 3*B, panel c*) were lower in *Plin5*$^{-/-}$ mice than wild-type mice when the animals were fed. In contrast, contents of TAG and FA were higher in *Plin5*$^{-/-}$ mice than wild-type mice when they were fasted. Thus, under fasting conditions, where Plin5 expression is abundant in the liver (4), the effect of Plin5 ablation on lipid accumulation was apparently opposite that in the heart. In BAT, TAG content was significantly lower for *Plin5*$^{-/-}$ mice than wild-type mice when they were fed (Fig. 3*A, panel d*). This difference was not observed when mice were fasted, due to the severe reduction in TAG that occurred only in wild-type mice. No difference was observed in the tolerance to cold exposure between the two genotypes (data not shown), despite the different TAG content in the fed state. Inguinal WAT contained indistinguishable levels of TAG in both genotypes of mice, although they were significantly decreased by fasting (Fig. 3*A, panel e*). Liver, BAT, and WAT contained abundant or large LDs in both genotypes (data not shown). Thus, the effect of Plin5 ablation was most prominently revealed as apparent lack of LDs only in the heart.

Blood Parameters and Other Systemic Effects of Plin5 Ablation—Blood nonesterified fatty acid levels were 1.4-fold higher in *Plin5*$^{-/-}$ mice than in wild-type mice in the fasted state (data not shown). This result, although the underlying mechanism is not clear, suggests that the absence of detectable LDs in the hearts of *Plin5*$^{-/-}$ mice is not due to decreased delivery of FA to the heart. No difference was noted between the two genotypes in blood concentrations of glucose, TAG, ketone body, and insulin (data not shown).

Food intake did not differ significantly between wild-type and *Plin5*$^{-/-}$ mice (Fig. 4*A*). *Plin5*$^{-/-}$ mice consumed 7% more oxygen than wild-type mice during the dark period (Fig. 4*B*). The respiratory quotient was similar between *Plin5*$^{-/-}$ and wild-type mice during either light or dark (Fig. 4*C*). The locomotor activity of *Plin5*$^{-/-}$ mice was higher than that of wild-type mice during the dark phase (Fig. 4*D*), being consistent with increased respiration. As shown in Fig. 9, fatty acid oxidation is enhanced in the hearts of *Plin5*$^{-/-}$ mice. This would yield more ATP in the hearts, hence apparently being consistent with the increased locomotor activity. The mechanism of behavioral change caused by the ablation of Plin5 needs to be addressed.

Intracellular Distribution of TAG and LD-binding Proteins in the Heart—Based on the marked effect of Plin5 ablation on heart LDs, we focused our further study on this organ. As shown in Fig. 3*A, panel a*, a substantial amount of TAG was contained in the hearts of *Plin5*$^{-/-}$ mice, despite the apparent lack of LDs. We asked where the remaining TAG was located in the heart cells, by subcellular fractionation employing sucrose-density gradient centrifugation. In wild-type samples, TAG was

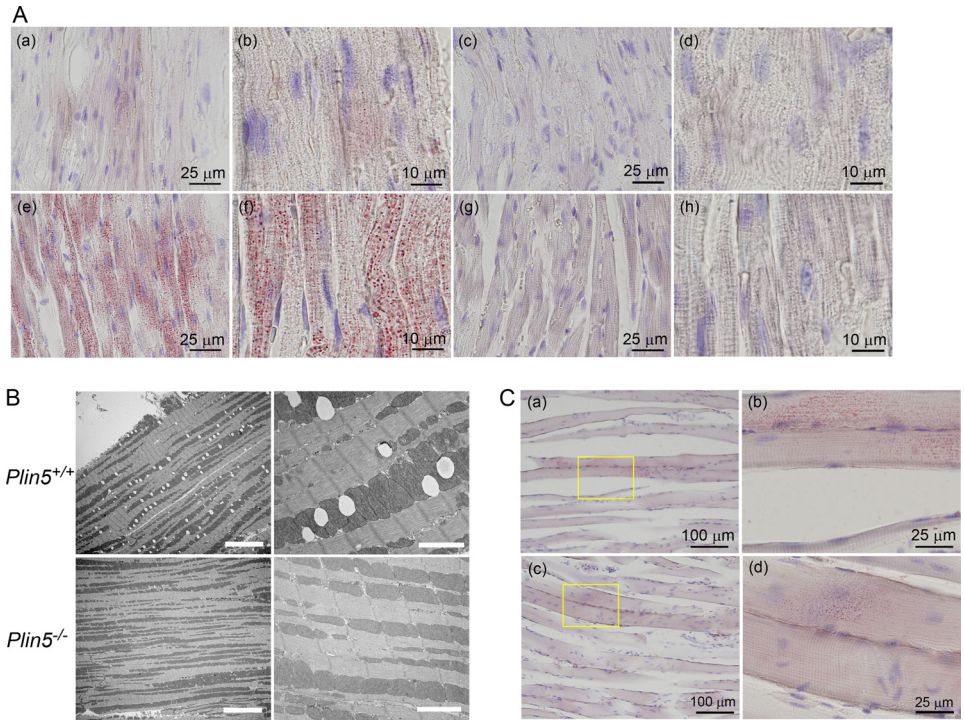

FIGURE 2. **Absence of LDs in the hearts of *Plin5*$^{-/-}$ mice.** *A*, ORO staining of heart cryosections of wild-type (*panels a*, *b*, *e*, and *f*) and *Plin5*$^{-/-}$ (*panels c*, *d*, *g*, and *h*) mice in the fed (*panels a–d*) and fasted (*panels e–h*) states. *Panels a*, *c*, *e*, and *g*, low magnification (*bar*, 25 μm). *Panels b*, *d*, *f*, and *h*, high magnification (*bar*, 10 μm). No LD was observed even by close inspection of the sections of *Plin5*$^{-/-}$ mice in either state. In wild-type mice, out of 20 randomly selected microscopic fields (each 86.4 × 60.5 μm), four in the fed state and all in the fasted state contained detectable LDs. The number of LDs in a field was 18.7 ± 11.0 in the fed mice and 966 ± 409 in the fasted mice, respectively ($p = 4.3 \times 10^{-9}$). The sizes of LDs were 0.22 ± 0.04 μm in the fed and 0.64 ± 0.11 μm in the fasted states, respectively ($p = 2.3 \times 10^{-7}$). *B*, representative electron microscopic images of the hearts of wild-type and *Plin5*$^{-/-}$ mice fasted overnight. *Left panels*, low magnification (*bar*, 10 μm), and *right panels*, high magnification (*bar*, 2 μm). Note that LDs are observed as *white ovals* only in wild-type mice. *C*, ORO staining of soleus muscle cryosections. *Panels a* and *b*, wild-type, and *panels c* and *d*, *Plin5*$^{-/-}$ mice, both fasted overnight. *Panels a* and *c*, low magnification. *Bar*, 100 μm. *Panels b* and *d*, high magnification of the area enclosed by a *rectangle*. *Bar*, 25 μm.

mostly recovered in the upper fraction under fasted conditions and also to a considerable extent under fed conditions (Fig. 5*A*). However, TAG was undetectable in the upper fraction in the hearts of *Plin5*$^{-/-}$ mice under both fed and fasted conditions, being consistent with the apparent lack of LDs. Instead, TAG was only found in the lower fractions, most abundantly in the pellet (fraction 9) in *Plin5*$^{-/-}$ mice. Even for wild-type mice, a substantial amount of TAG was recovered in the lower fractions, the pellet in particular, when they were fed.

In wild-type mice, although Plin5 was detectable in the upper fraction, it was found to a much larger extent in the lower fractions, particularly the pellet (Fig. 5*B*). Conversely, Plin2 was abundant in the upper fraction in the fasted state but was mostly recovered in the lower fractions particularly just above the pellet (fraction 8) in the fed state. Thus, the distribution of these two proteins was different in that Plin5 was less abundant in the upper fraction, although pelleted to a larger extent, as compared with Plin2. In *Plin5*$^{-/-}$ mice, Plin2 was recovered only in the lower fractions irrespective of feeding conditions. Proteins (Fig. 5*C*) as well as organellar and cytosolic markers (Fig. 5*D*) were also abundant in the lower fractions, with most concentrated just above the pellet (fraction 8). Actin was pelleted under the same conditions to a significant extent. These results suggest that TAG as well as perilipin proteins are mostly contained in denser structures, in the hearts of *Plin5*$^{-/-}$ mice and fed wild-type mice. These structures are probably different from major organelles such as mitochondria and endoplasmic reticulum, based on the different distribution in sucrose gradient.

To further characterize the TAG-containing dense structures, we performed another centrifugal experiment with a wider range of sucrose gradient. In both fed wild-type and *Plin5*$^{-/-}$ mice, TAG was distributed in the fractions in a density range of 1.18–1.22 (Fig. 5*E*), overlapping with the distribution of mitochondria and, to a lesser extent, endoplasmic reticulum (Fig. 5*F*). Plin5 and Plin2 were found in these fractions and also less dense fractions where endoplasmic reticulum was abundant. This result suggests that TAG is contained in structures with defined densities in the hearts of fed wild-type and *Plin5*$^{-/-}$ mice, although these structures were not separated from other organelles in this centrifugal condition.

We next examined the distribution of perilipin proteins in the heart cells by immunofluorescence microscopy. Plin5 and Plin2 coexisted in particulate structures in the hearts of wild-type mice (Fig. 6, *A–D*), consistent with previous observations (5, 28). Relative abundance of these proteins on individual particles was not necessarily constant, as judged by the different color tones of particles in merged views (Fig. 6, *C* and *D*). Even for fed mice, Plin5 and Plin2 extensively coexisted in particulate structures in most heart cells (Fig. 6*A*), although most of these particulates appeared significantly smaller than those in fasting mice (Fig. 6*B*). The abundance of these structures in fed mice was in contrast to the limited occurrence of LDs in a small population of cells revealed by ORO staining (Fig. 2*A*). For fast-

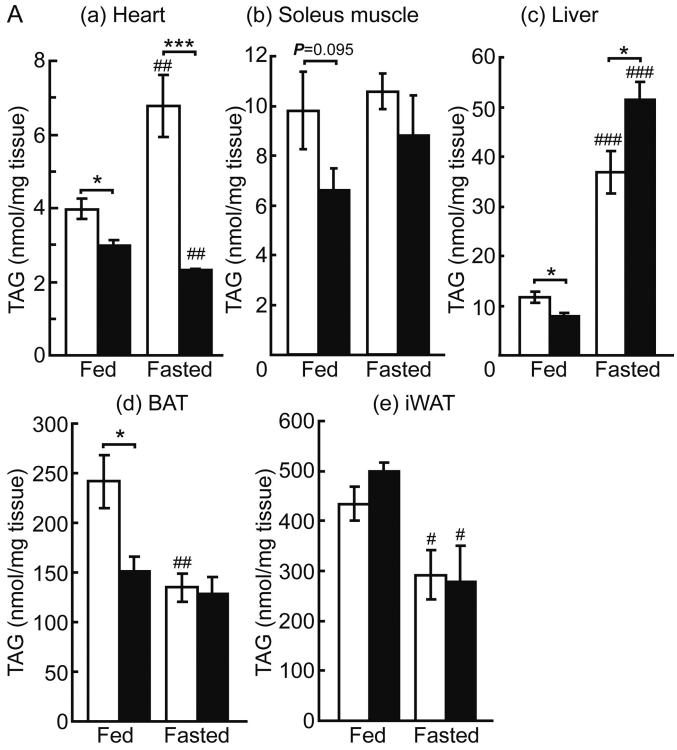

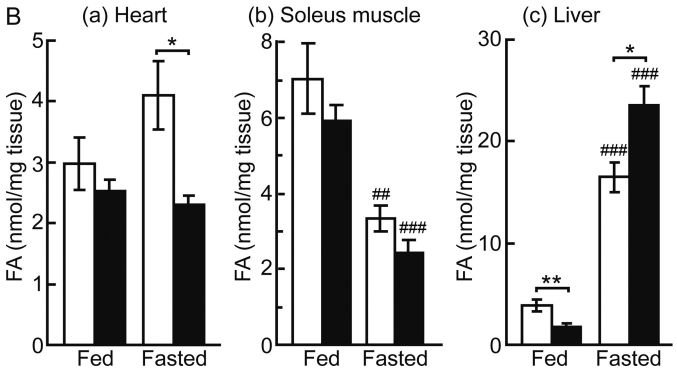

FIGURE 3. **TAG and FA contents in the tissues of fed and fasted wild-type and *Plin5*$^{-/-}$ mice.** *A*, TAG content in the heart (*panel a*), soleus muscle (*panel b*), liver (*panel c*), BAT (*panel d*), and inguinal WAT (*panel e*) (n = 5–8 per group). *B*, free FA content in the heart (*panel a*), soleus muscle (*panel b*), and liver (*panel c*) (n = 5–8 per group). *Open bars*, wild-type mice, and *filled bars*, *Plin5*$^{-/-}$ mice. ***, $p < 0.001$; **, $p < 0.01$; *, $p < 0.05$; ###, $p < 0.001$; ##, $p < 0.01$; #, $p < 0.05$, against fed animals of the same genotypes.

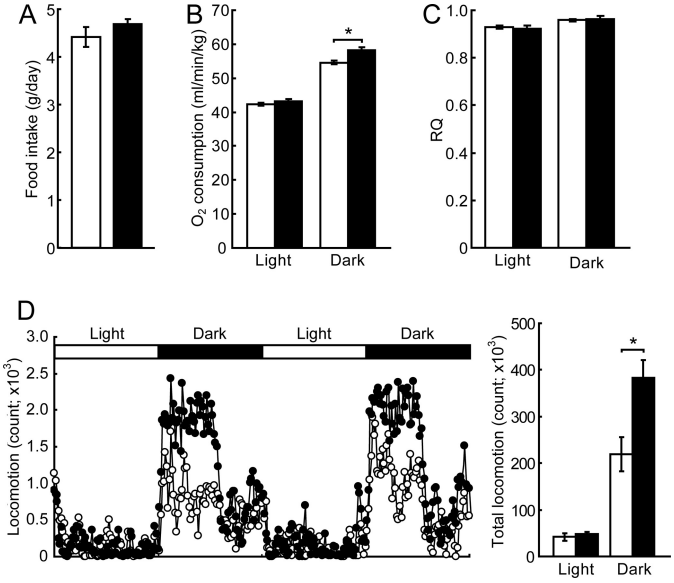

FIGURE 4. **Energy metabolism of *Plin5*$^{-/-}$ mice.** *A*, food intake. Mice were housed individually for 10 days, and food intake per day was measured (n = 10 per group). *B*, oxygen consumption. *C*, respiratory quotient (n = 6 per group). *D*, locomotion of *Plin5*$^{-/-}$ mice. Dot-plot demonstrates the time course of locomotor activity during 2 days. Each *dot* is the mean of locomotion of six mice. The *graph* on the *right* represents the total counts of locomotion during the experiment. *, $p < 0.05$.

ing wild-type mice, many of the particulates positive for Plin5 and Plin2 exhibited ring-shaped images typical of LDs (Fig. 6*D*). These structures were also positive for lipid staining with Bodipy (132 of 147 Plin5-positive particles being Bodipy-positive) (Fig. 6*F*). For fed wild-type mice, however, the particles were rarely ring-shaped (Fig. 6*C*) and mostly devoid of lipid staining (only 8 of 132 Plin5-positive particles being Bodipy-positive) (Fig. 6*E*). We obtained similar immunostaining patterns with another lot of anti-Plin5 antibody (data not shown). These results suggest that most of the particles carrying Plin5 and Plin2 in the hearts of fed wild-type mice represent very small LDs with low lipid contents. They are hardly detectable in conventional microscopy, because they are not stained with ORO. In the hearts of *Plin5*$^{-/-}$ mice, no LDs were detected by Bodipy staining (Fig. 6, *G* and *H*), but, interestingly, Plin2 still exhibited punctate staining irrespective of feeding conditions (Fig. 6, *I* and *J*).

We examined the effect of Plin5 ablation on the expression of other perilipin proteins and lipases. Among them, Plin2 protein expression in the heart was significantly decreased upon Plin5 ablation (Fig. 7*A*). However, expression of Plin2 mRNA was not significantly affected by Plin5 ablation (Fig. 7*B*), indicating the involvement of a post-transcriptional event in the decrease of Plin2 protein. Previous studies found Plin2 protein to be degraded by proteasomes under conditions where Plin2 was not stabilized by binding to LDs or lipids (29, 30). Thus, it is conceivable that Plin2 does not compensate for the ablation of Plin5 in supporting LDs to be detectable but is rather degraded to a large extent in the hearts of *Plin5*$^{-/-}$ mice. However, as suggested by immunofluorescence microscopy (Fig. 6, *I* and *J*), the remaining Plin2 was still located on particulate structures, even though LDs were undetectable by electron microscopy or lipid staining. mRNA expression of Plin3, ATGL, and HSL was slightly affected by Plin5 ablation (Fig. 7*B*), but their protein amounts did not differ between the two genotypes (Fig. 7*A*).

Plin5 Maintains LDs by Restricting Lipase(s)—Perilipin family proteins have generally been suggested to protect LDs from attack by lipases (17). Hence, we supposed that the apparent lack of LDs in the hearts of *Plin5*$^{-/-}$ mice is due to the loss of this function. To examine this notion, we tried to inhibit lipase(s), particularly ATGL, a major lipase of the heart, in the intact organ. For this purpose, the hearts of *Plin5*$^{-/-}$ mice were briefly perfused with BEL, a potent inhibitor of the iPLA$_2$ family of phospholipases/lipases, including ATGL (31). This treatment effectively eliminated the BEL-sensitive lipase activities in the heart in both genotypes of mice, as confirmed by an *in vitro* lipase assay (Fig. 8*A*). Importantly, the ratio of lipase activity remaining after the treatment in wild-type mice (70%) was

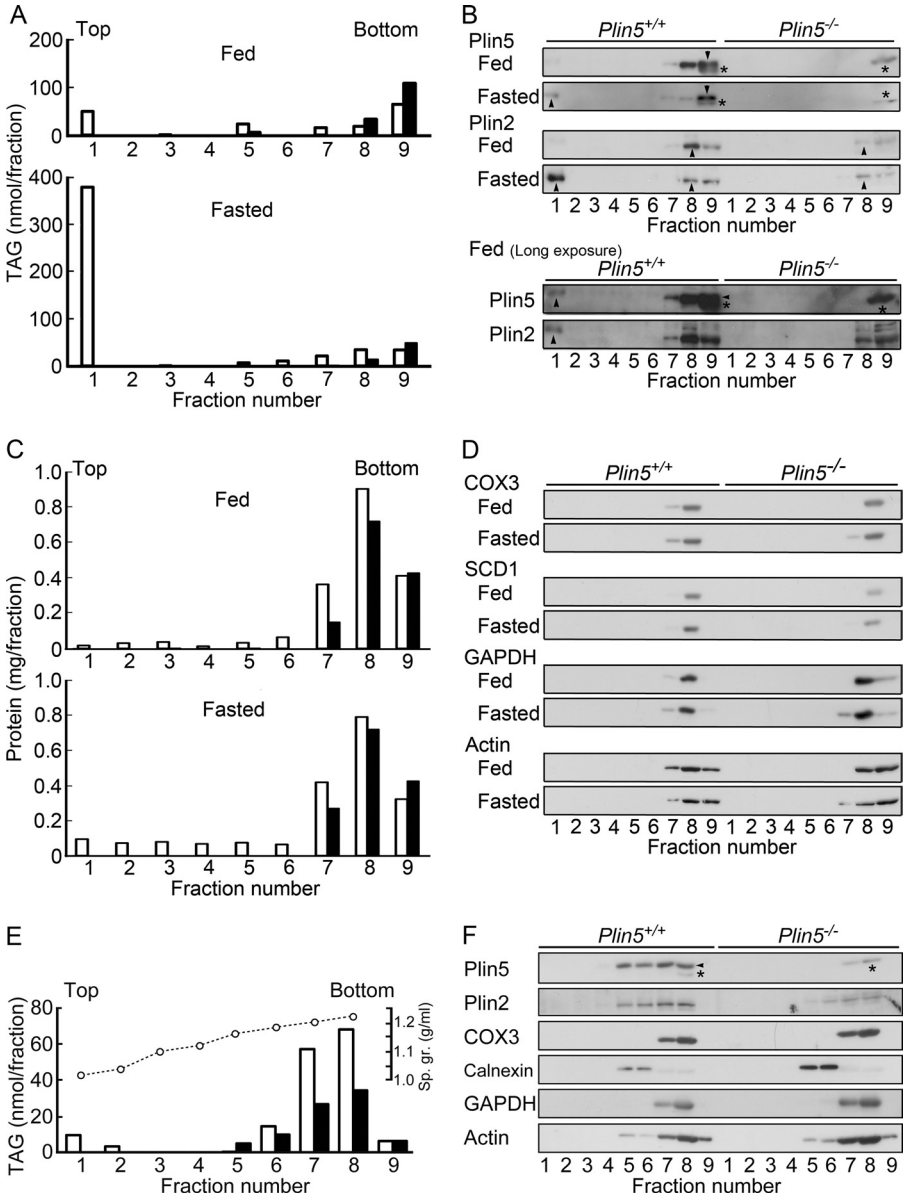

FIGURE 5. **Subcellular fractionation of heart homogenates.** *A*, TAG content in the fractions obtained by sucrose density gradient centrifugation of heart homogenates of wild-type and *Plin5*$^{-/-}$ mice under fed and fasted conditions. *Open bar*, wild-type mice, and *filled bar*, *Plin5*$^{-/-}$ mice. *B*, immunoblotting of Plin5 and Plin2 in the fractions of *A*. For fed animals, results of long exposure of the blots are also shown. *Arrowhead*, Plin5 and Plin2. *Asterisk*, nonspecific band, which was not recognized by another lot of anti-Plin5 antibody (Progen) raised against the same carboxyl-terminal epitope. *C*, protein contents in the same fractions. *D*, distribution of markers of mitochondria (cytochrome *c* oxidase subunit 3 (*COX3*)), endoplasmic reticulum (stearoyl-CoA desaturase 1 (*SCD1*)), and cytosol (glyceraldehyde-3-phosphate dehydrogenase (*GAPDH*)), and actin filament through the gradients. *E*, TAG content in the fractions after centrifugation through a wider sucrose-density gradient. Heart homogenates from fed wild-type (*open bar*) and *Plin5*$^{-/-}$ (*filled bar*) mice were analyzed. *Open circle*, specific gravity (*Sp. gr.*) of each fraction. *F*, distribution of Plin5, Plin2, and marker proteins in the same fractions as in *E*. Calnexin was used as a marker of endoplasmic reticulum.

comparable with the ratio of remaining heart lipase activity in ATGL-KO mice (23). Interestingly, the BEL-sensitive lipase activity was significantly lower in the hearts of *Plin5*$^{-/-}$ mice than that of wild-type mice, despite the similar ATGL protein level in both genotypes of mice (Fig. 7*A*). After BEL perfusion, LDs were observed in the hearts of *Plin5*$^{-/-}$ mice as abundantly as in wild-type mice (Fig. 8*B*). The amount of Plin2 relative to that of an internal control, GAPDH, was also recovered by the perfusion, to a level close to that in wild-type mice (Fig. 8*C*). Moreover, the TAG content in the hearts of *Plin5*$^{-/-}$ mice was increased by the treatment, reaching a level indistinguishable from that of wild-type mice without the inhibitor (Fig. 8*D*). Thus, detectable LDs as well as lipid accumulation was recovered by inhibiting ATGL and related lipases in the hearts of *Plin5*$^{-/-}$ mice. This result indicates that Plin5 maintains LDs in the heart by blocking the actions of ATGL and possibly other lipase(s).

Plin5 Deficiency Promotes Fatty Acid Oxidation in Cardiomyocytes—We next asked how FA is managed in the hearts of *Plin5*$^{-/-}$ mice, where it is poorly sequestered as TAG. To address this issue, FA oxidation was monitored with cultured cardiomyocytes. For convenience, hearts from mice 1.5–3 days after birth, in which Plin5 and FA oxidation enzymes were fully expressed (Fig. 9*A*), were used. Expression of those

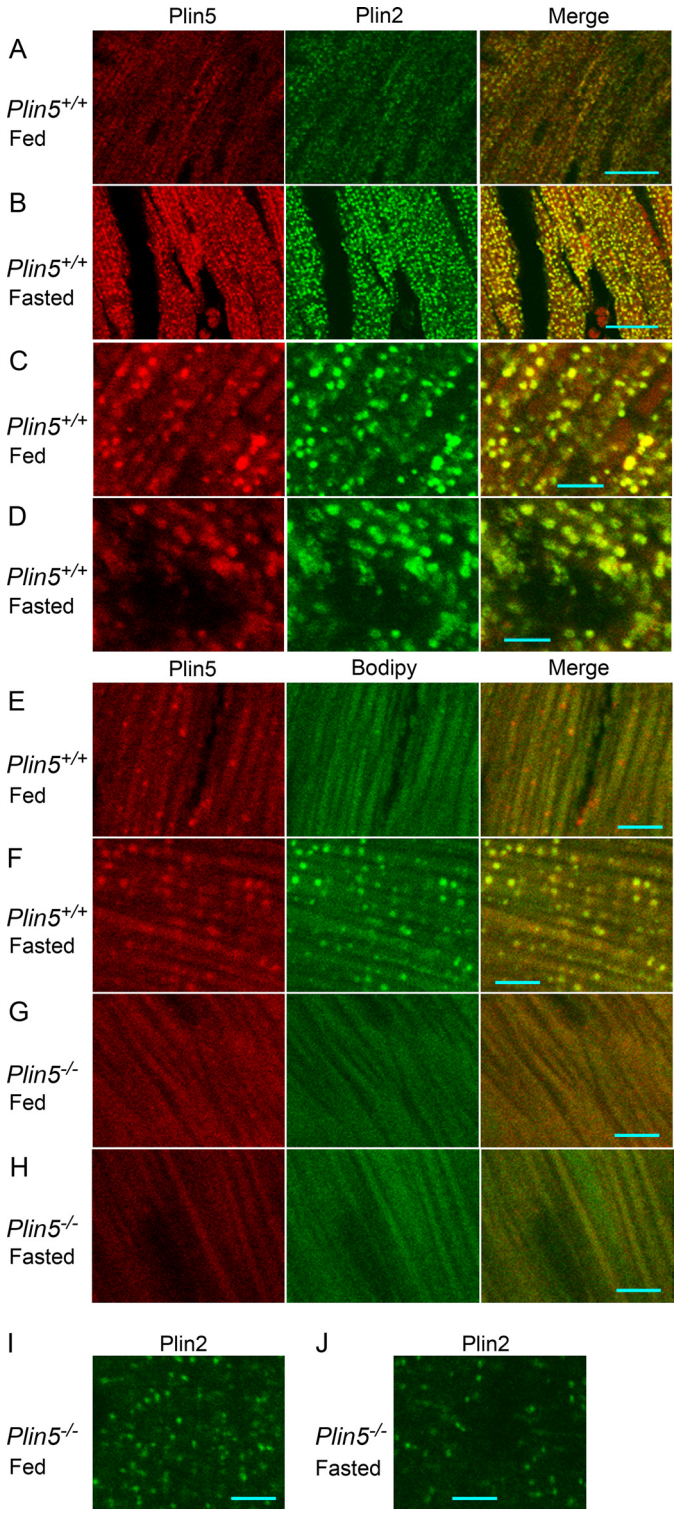

FIGURE 6. **Immunofluorescence staining of heart sections**. *A–D*, immunofluorescence staining of Plin5 and Plin2 in heart sections from wild-type mice. *A* and *C*, fed mice; and *B* and *D*, starved mice. *A* and *B*, low magnification. *Bar*, 20 μm. *C* and *D*, high magnification. *Bar*, 5 μm. *E–H*, double staining with an anti-Plin5 antibody and Bodipy 493/503. Cryosections of the hearts of wild-type (*E* and *F*) and *Plin5*$^{-/-}$ (*G* and *H*) mice under fed (*E* and *G*) and fasted (*F* and *H*) conditions were stained. *I* and *J*, immunostaining of Plin2 in *Plin5*$^{-/-}$ mice under fed (*I*) and fasted (*J*) conditions. *Bar*, 5 μm.

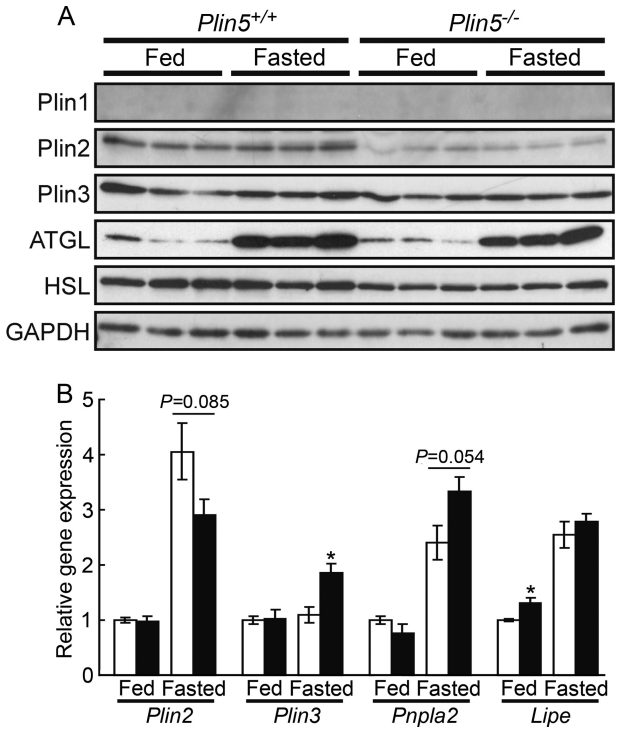

FIGURE 7. **Expression of perilipin family proteins and lipases in the heart.** *A*, immunoblotting of the proteins (three animals for each group). *B*, quantitative RT-PCR of mRNAs. Signal intensities were corrected based on that of *Rplp0* (36B4) ($n = 5$ per group). *Open bar*, wild-type mice, and *filled bar*, *Plin5*$^{-/-}$ mice. *, $p < 0.05$, against wild-type mice under the same feeding condition. *Pnpla2* and *Lipe* denote the genes of ATGL and HSL, respectively.

proteins and lipases was largely retained during the culture (Fig. 9*B*). In *Plin5*$^{-/-}$ cells, the radioactivity of palmitic acid was significantly better incorporated into CO_2 (Fig. 9*C*). Production of intracellular ASM (Fig. 9*D*), which represent active metabolites such as acetyl-CoA and tricarboxylic acid cycle intermediates (32), was also increased in *Plin5*$^{-/-}$ cells. However, radioactivity in extracellular ASM, probably representing products excluded from active metabolism, was not changed by deletion of Plin5 (Fig. 9*E*). Etomoxir is a specific inhibitor of carnitine *O*-palmitoyltransferase type 1, an enzyme required for the translocation of fatty acyl-CoA into mitochondria. This agent significantly, albeit partially, inhibited the production of radioactive CO_2 and intracellular ASM (Fig. 9, *C* and *D*). It was reported that in the mice intraperitoneally injected with etomoxir, CPT1 activity was decreased only by 40% in the heart and nearly completely in the liver and skeletal muscle (33), although the reason was not defined. Thus, it is conceivable that mitochondria make a major contribution to FA oxidation in this experimental setting, although the contribution of peroxisomal FA oxidation activity would not be neglected. Total incorporation of FA was not different between *Plin5*$^{-/-}$ and wild-type cells (Fig. 9*F*). Thus, impaired TAG accumulation in the hearts of *Plin5*$^{-/-}$ mice is not due to decreased uptake of FA. Taken together, these results suggest that FA is rapidly oxidized in mitochondria in the hearts of *Plin5*$^{-/-}$ mice, rather than being retained as TAG.

Plin5 Deficiency Increases Oxidative Stress to the Heart—Enhanced fatty acid oxidation may lead to increased production of ROS (34), a mediator of lipotoxicity. Accordingly, we estimated ROS production in the hearts of wild-type and *Plin5*$^{-/-}$ mice by measuring the content of lipid peroxide, a product of peroxidative action by ROS. The level of lipid peroxide was signifi-

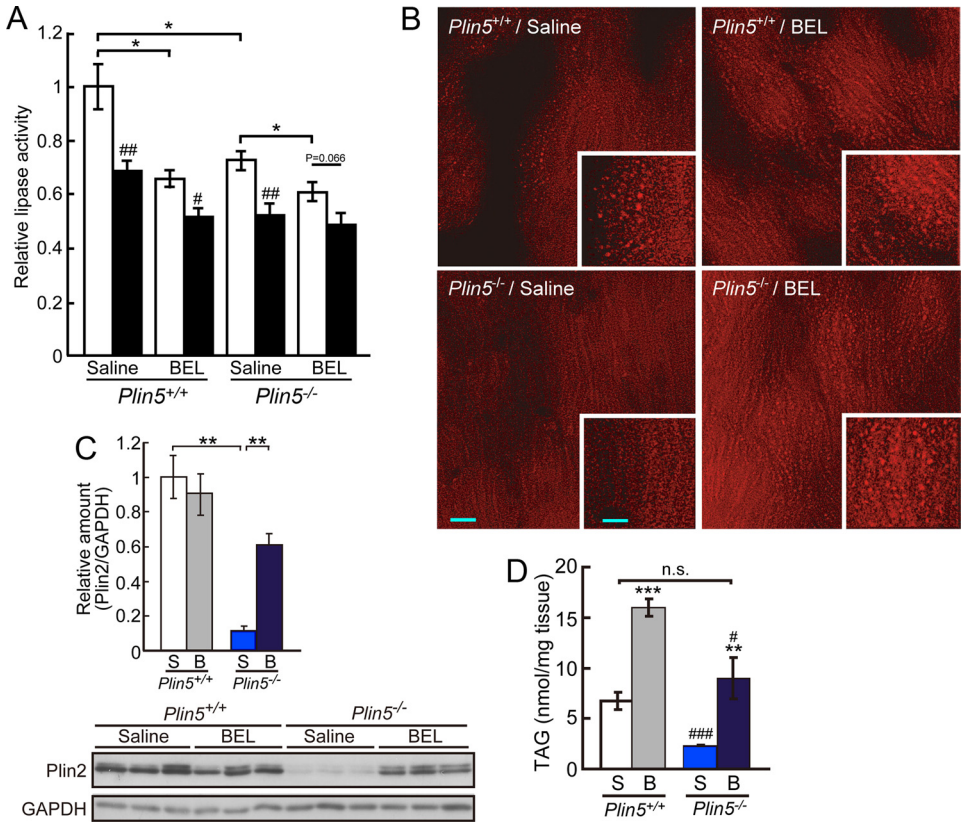

FIGURE 8. **Plin5 maintains LDs by restricting lipases.** *A*, decrease in heart lipase activities by the perfusion with BEL. Lipase activities were measured with the heart homogenates of mice perfused with saline or BEL ($n = 3–4$ per group). Assays were performed in the absence (*open bar*) or presence (*filled bar*) of 50 μM BEL. Relative enzyme activities taking the value of saline-treated wild-type mice measured without BEL (14.1 nmol of oleic acid released/h/mg of protein) as 1. *, $p < 0.05$; ##, $p < 0.01$; #, $p < 0.05$, against values obtained without BEL during the assay for the same genotypes of mice with the same treatment. *B*, effect of BEL perfusion on the occurrence of LDs in the hearts of wild-type and *Plin5*$^{-/-}$ mice. Representative images of Nile Red-stained frozen sections are shown. *Bar*, 10 μm. *Inset*, high magnification view. *Bar*, 5 μm. Results were confirmed for several microscopic fields obtained from at least two animals for each group. *C*, effect of BEL on the protein content of Plin2 in the heart. *Top*, relative amount of Plin2 normalized with that of GAPDH in the heart lysates from the same animals as in *A* ($n = 3$), estimated from the result of immunoblotting (*bottom*). *S*, saline-treated, and *B*, BEL-treated. **, $p < 0.01$. *D*, effect of BEL on TAG content in the heart ($n = 5–8$ per group). ***, $p < 0.001$; **, $p < 0.01$, against saline-treated animals of the same genotype. ###, $p < 0.001$; #, $p < 0.05$, against wild-type mice with the same treatment. *n. s.*, difference not significant.

cantly higher in the hearts of *Plin5*$^{-/-}$ mice than that of wild-type mice at both 16–20 and 30–38 weeks of age, although the values increased with age in both genotypes (Fig. 10*A*). NAC is a precursor of glutathione, a substrate for glutathione peroxidase, and is often used to alleviate oxidative stress (35). The mice were continuously given this agent from 16 to 18 weeks to the day of experiment at 30–32 weeks of age. By this treatment, the heart content of lipid peroxide was lowered in *Plin5*$^{-/-}$ mice to a level close to that of younger wild-type mice. This result indicates that NAC indeed counteracted the increased action of ROS in the hearts of *Plin5*$^{-/-}$ mice in this experimental setting.

The increase in oxidative stress may affect the contractile function of the hearts of *Plin5*$^{-/-}$ mice. This possibility was examined by echocardiography, using mice 16–18 and 30–38 weeks old (Fig. 10*B*). End-diastolic dimension (LVID;d) and end-systolic dimension (LVID;s) were enlarged, and FS was reduced in the aged *Plin5*$^{-/-}$ mice but not in wild-type mice (Fig. 10*C*). These values returned to normal in the aged *Plin5*$^{-/-}$ mice on treatment with NAC from 16 to 18 to 30–32 weeks. In the regression analysis for the aged mice, lipid peroxide levels in the hearts of individual animals correlated well with LVID;d and LVID;s and moderately with FS (Fig. 10*D*). The correlation between FS and the lipid peroxide level was apparently lower, because FS was derived from LVID;d and LVID;s by calculation, which unavoidably expands variations. Hence, ablation of Plin5 leads to further weakening of heart function with age, and the cumulative effects of increased oxidative stress are likely to contribute to this.

DISCUSSION

One of the most striking observations from *Plin5*$^{-/-}$ mice is that *Plin5*$^{-/-}$ mice lacked detectable LDs only in the heart. Consistent with the apparent lack of LDs, the hearts of *Plin5*$^{-/-}$ mice contained significantly less TAG and FA, as compared with that of wild-type mice. LDs were recovered upon brief perfusion of the heart with an inhibitor of ATGL and related lipases. This result indicates that Plin5 antagonizes lipase actions, consistent with observations that perilipin family members, including Plin5, protect TAG from attack by lipases (5, 6, 17). Several recent reports (28, 36) suggested that Plin5 serves as a platform for the interaction of ATGL with CGI-58 on the LD surface, thus facilitating lipolysis. Another group reported that Plin5 interacts with ATGL and inhibits the enzymatic activity (37). Data from this study suggest that the func-

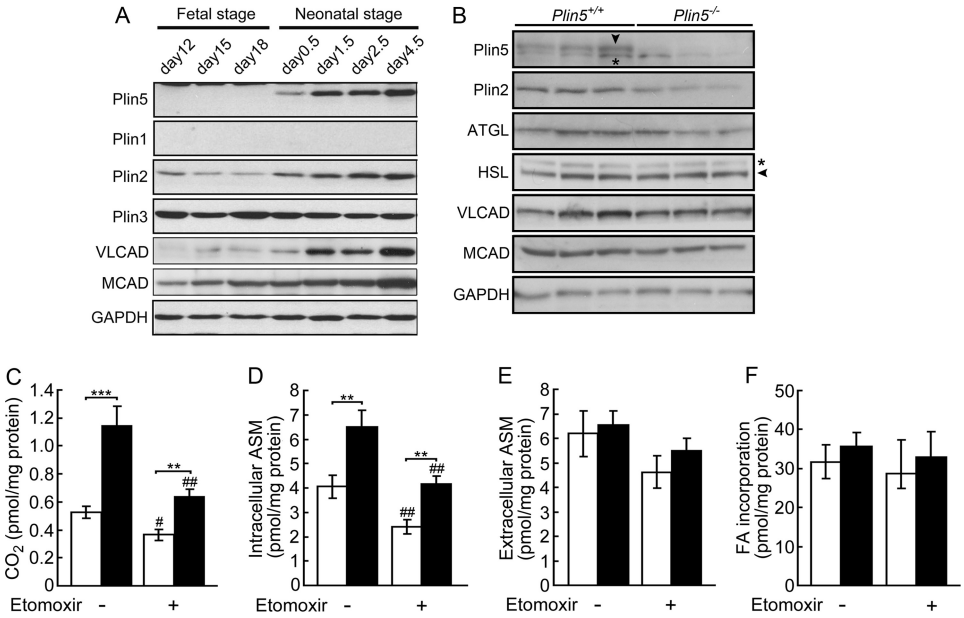

FIGURE 9. **Lack of Plin5 promotes FA oxidation in cardiomyocytes.** *A*, expression of perilipin family proteins and fatty acid oxidation enzymes in the hearts of wild-type mice before and after birth. *VLCAD*, very long-chain acyl-CoA dehydrogenase, and *MCAD*, medium-chain acyl-CoA dehydrogenase. *B*, expression of perilipin family proteins, lipases, and fatty acid-oxidizing enzymes in cardiomyocytes after the culture for 2 days in the presence of oleic acid (see "Experimental Procedures"). Cardiomyocytes prepared from the hearts of eight wild-type and *Plin5*$^{-/-}$ mice 3 days after birth were seeded in three culture dishes, respectively. *Arrowhead*, correct band of Plin5 and HSL. *, nonspecific band. *C–E,* FA oxidation by cardiomyocytes as assessed by conversion of [^{14}C]palmitic acid to CO_2 (*C*), intracellular ASM (*D*), and extracellular ASM (*E*). *F*, total incorporation of FA. *Open bar*, wild-type mice, and *filled bar*, *Plin5*$^{-/-}$ mice. The assay was performed with or without etomoxir. $n = 8–9$ representing the number of independent experiments per group. In each experiment, values obtained with three culture dishes were averaged. ***, $p < 0.001$; **, $p < 0.01$; ##, $p < 0.01$; #, $p < 0.05$, against etomoxir-untreated cells of the same genotype.

tion of Plin5 in the heart is to impede, rather than assist, lipolysis.

LDs were observed in other tissues, including skeletal muscle, the liver, BAT, and WAT of *Plin5*$^{-/-}$ mice. The content of TAG was decreased in the liver and BAT of fed *Plin5*$^{-/-}$ mice, as compared with wild-type mice. Interestingly, in the fasted state, the liver of *Plin5*$^{-/-}$ mice contained more TAG and FA than that of wild-type mice, in contrast to the case of the heart. These results suggest that roles of Plin5 as well as LDs may differ, depending on the functions of individual cell and tissue types. It is also possible that the unique combinations of Plin5 with other LD proteins, including the perilipin family members, confer tissue-specific function. Plin5 is more protective than Plin2, another major perilipin protein in the heart, according to previous observations (37, 38). We also confirmed it by an experiment in which we expressed Plin5 or Plin2, with or without ATGL, in cultured cells (data not shown). The protective function of Plin5 in the heart is not substituted for by other proteins, including Plin2, probably due to highly active lipid metabolism. In fact, the resting metabolic rate on a fat-free mass basis is much higher in the heart than in most other organs, including skeletal muscle and the liver (39). Moreover, 60–70% of energy is supplied by FA in the heart (20). Thus, at least under sedentary conditions, lipid metabolism is more moderate in tissues other than the heart. Hence, other proteins may effectively compensate for a deficiency of Plin5 to maintain detectable LDs in those tissues.

In this study, the occurrence of very small LDs in the hearts of fed wild-type mice was suggested by immunofluorescence microscopy and subcellular fractionation. These structures seem to be under the limit of detection with ORO or Bodipy, because of their small size and low lipid content. They would not float, but rather sediment, upon centrifugation under the usual conditions for LD isolation, due to their higher protein to lipid ratio. A precedent of dense protein-lipid complex is plasma high density lipoprotein. Its density ranges 1.063–1.210 (40), overlapping the density 1.09–1.10 at the bottom in the present fractionation experiment (Fig. 5, *A* and *B*). We confirmed that they are indeed structures with defined densities by a centrifugal experiment employing a wider range of sucrose gradients (Fig. 5, *E* and *F*).

Plin5 and Plin2 did not seem to coat LDs evenly in immunofluorescence microscopy of the heart. In subcellular fractionation, Plin5 tended to be less concentrated in the upper fractions, and more abundant in the lower fractions, particularly the pellet, as compared with Plin2. Thus, Plin5 seems to be more abundant in smaller LDs as compared with Plin2. Occurrence of immature LDs abundant in Plin5 in cultured cells as well as the heart and liver was reported very recently (41). Thus, it is conceivable that Plin5 is particularly important for protecting very small LDs that have larger relative surface areas from lipase attack. Involvement of Plin5 in the interaction between LDs and mitochondria was shown recently (42). In this cell fractionation study, the distribution of Plin5 partially overlapped that of mitochondria, possibly being consistent with the report.

In the hearts of *Plin5*$^{-/-}$ mice, Plin2 exhibited a punctate distribution in immunofluorescence microscopy. Moreover, TAG was mostly recovered, and Plin2 was also to a large extent recovered in the pellet by subcellular fractionation (Fig. 5, *A* and *B*). Thus, it is conceivable that, Plin2-coated minute LDs still occur in the hearts of *Plin5*$^{-/-}$ mice, despite the apparent lack

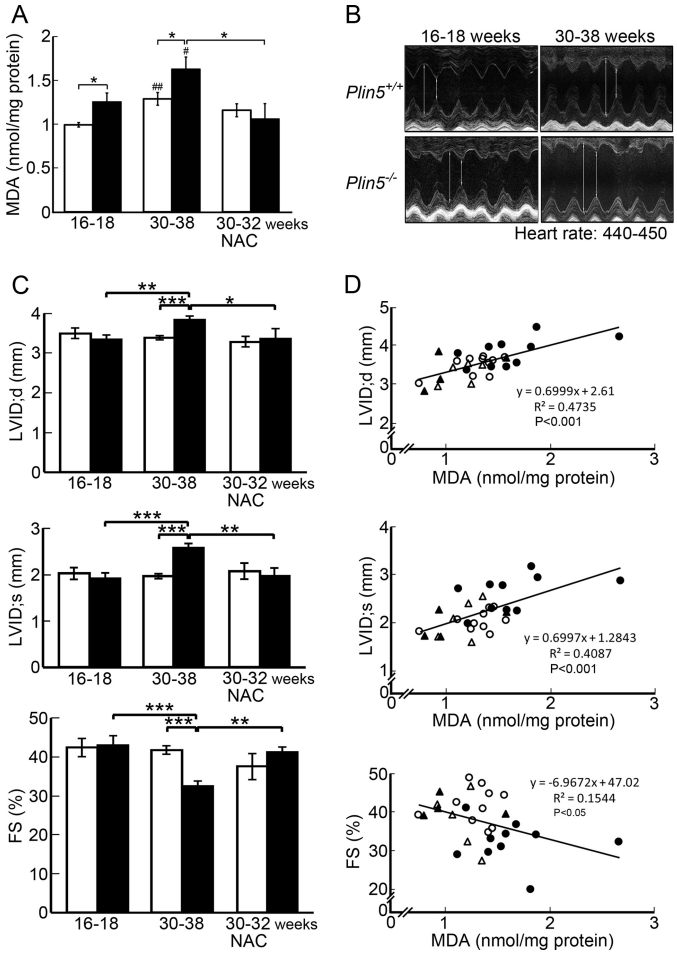

FIGURE 10. **Plin5 deficiency enhances oxidative burden in the heart, causing a functional decline.** *A*, evaluation of ROS generation by TBARS assay. Malondialdehyde (*MDA*) was quantified colorimetrically to monitor lipid peroxidation. Measurements were performed on the hearts from mice at 16–18 weeks ($n = 9$), 30–38 weeks ($n = 10$), and mice continuously treated with NAC from 16 to 18 weeks of age to the day of the experiment at 30–32 weeks of age ($n = 5$ for wild-type and 4 for *Plin5*$^{-/-}$ mice, respectively). *B*, representative images of echocardiography in age-matched mice (16–18 or 30–38 weeks old). *Long* and *short vertical lines* indicate LVID;d and LVID;s, respectively. *C*, values of LVID;d (*top panel*), LVID;s (*middle panel*), and FS (*bottom panel*) were evaluated from images of echocardiography, at heart rates of 440–450 beats/min. $n = 6$ for both genotypes at 16–18 weeks, 23 and 16 for wild-type and *Plin5*$^{-/-}$ mice at 30–38 weeks, respectively, and 5 and 4 for NAC-treated wild-type and *Plin5*$^{-/-}$ mice, respectively. *Open bar*, wild-type mice, and *filled bar*, *Plin5*$^{-/-}$ mice. ***, $p < 0.001$; **, $p < 0.01$; *, $p < 0.05$; ##, $p < 0.01$; #, $p < 0.05$, against the values of young mice of the same genotype. *D*, regression analysis of the correlations between the heart MDA content and LVID;d (*top panel*), LVID;s (*middle panel*), and FS (*bottom panel*). The first-order regression line was obtained by the least squares method from the data for individual mice. *Open* and *closed circles*, wild-type and *Plin5*$^{-/-}$ mice at 30–38 weeks, and *open* and *closed triangles*, NAC-treated wild-type and *Plin5*$^{-/-}$ mice, respectively.

of LDs. They are under the limit of detection by usual microscopic techniques, due to their small sizes. They are largely, but probably not completely, depleted of TAG due to the absence of Plin5. Hence, most, if not all, of TAG remaining in the hearts of *Plin5*$^{-/-}$ mice is conceivably accommodated in those minute LDs. TAG may also be retained in part in other cellular compartments such as mitochondria and endoplasmic reticulum, as suggested by a classical study (43). A recent finding also showed that TAG is even an intrinsic component of an enzyme complex, cytochrome *c* oxidase (44).

The *Plin5*$^{-/-}$ mice allow one to evaluate the physiological significance of LDs in the heart. The generation of ROS was significantly promoted in the hearts of *Plin5*$^{-/-}$ mice, as assessed by the elevated level of lipid peroxide. This is consistent with the enhanced mitochondrial oxidation of FA in *Plin5*$^{-/-}$ mice; $FADH_2$ generated during the β-oxidation of FA promotes the production of ROS, by reversing the electron flow from mitochondrial complex II to complex I, a major site of ROS production (34). It is widely recognized that ROS induce cardiac hypertrophy and cardiomyocyte dysfunction through oxidative damage and/or aberrant redox signaling (45). In echocardiography, *Plin5*$^{-/-}$ mice exhibited a greater decrease in heart function at older ages, as compared with wild-type mice. Continuous NAC treatment negated this, as well as lowered the level of lipid peroxide. Moreover, the heart parameters significantly correlated with lipid peroxide levels on an individual basis. Based on these results, we propose that an important function of Plin5 in the heart is to suppress excess ROS production by sequestering FA in TAG, thus reducing FA oxidation in mitochondria. This function is crucial for protecting the heart from eventual functional decline.

Acknowledgments—We thank Drs. R. Zechner and T. Koide for critical reading of the manuscript. We also thank Drs. Takashi Hashimoto and S. Yamaguchi for anti-VLCAD and anti-MCAD antibodies and Dr. J. Suzuki for technical advice on the TBARS assay.

REFERENCES

1. Schaffer, J. E. (2003) Lipotoxicity. When tissues overeat. *Curr. Opin. Lipidol.* **14,** 281–287
2. Brasaemle, D. L. (2007) Thematic review series. Adipocyte biology. The perilipin family of structural lipid droplet proteins. Stabilization of lipid droplets and control of lipolysis. *J. Lipid Res.* **48,** 2547–2559
3. Kimmel, A. R., Brasaemle, D. L., McAndrews-Hill, M., Sztalryd, C., and Londos, C. (2010) Adoption of perilipin as a unifying nomenclature for the mammalian PAT family of intracellular lipid storage droplet proteins. *J. Lipid Res.* **51,** 468–471
4. Yamaguchi, T., Matsushita, S., Motojima, K., Hirose, F., and Osumi, T. (2006) MLDP, a novel PAT family protein localized to lipid droplets and enriched in the heart, is regulated by peroxisome proliferator-activated receptor α. *J. Biol. Chem.* **281,** 14232–14240
5. Wolins, N. E., Quaynor, B. K., Skinner, J. R., Tzekov, A., Croce, M. A., Gropler, M. C., Varma, V., Yao-Borengasser, A., Rasouli, N., Kern, P. A., Finck, B. N., and Bickel, P. E. (2006) OXPAT/PAT-1 is a PPAR-induced lipid droplet protein that promotes fatty acid utilization. *Diabetes* **55,** 3418–3428
6. Dalen, K. T., Dahl, T., Holter, E., Arntsen, B., Londos, C., Sztalryd, C., and Nebb, H. I. (2007) LSDP5 is a PAT protein specifically expressed in fatty acid-oxidizing tissues. *Biochim. Biophys. Acta* **1771,** 210–227
7. Martinez-Botas, J., Anderson, J. B., Tessier, D., Lapillonne, A., Chang, B. H., Quast, M. J., Gorenstein, D., Chen, K. H., and Chan, L. (2000) Absence of perilipin results in leanness and reverses obesity in Lepr(db/db) mice. *Nat. Genet.* **26,** 474–479
8. Tansey, J. T., Sztalryd, C., Gruia-Gray, J., Roush, D. L., Zee, J. V., Gavrilova, O., Reitman, M. L., Deng, C. X., Li, C., Kimmel, A. R., and Londos, C. (2001) Perilipin ablation results in a lean mouse with aberrant adipocyte lipolysis, enhanced leptin production, and resistance to diet-induced obesity. *Proc. Natl. Acad. Sci. U.S.A.* **98,** 6494–6499
9. Sztalryd, C., Xu, G., Dorward, H., Tansey, J. T., Contreras, J. A., Kimmel, A. R., and Londos, C. (2003) Perilipin A is essential for the translocation of hormone-sensitive lipase during lipolytic activation. *J. Cell Biol.* **161,** 1093–1103
10. Lass, A., Zimmermann, R., Haemmerle, G., Riederer, M., Schoiswohl, G., Schweiger, M., Kienesberger, P., Strauss, J. G., Gorkiewicz, G., and Zech-

ner, R. (2006) Adipose triglyceride lipase-mediated lipolysis of cellular fat stores is activated by CGI-58 and defective in Chanarin-Dorfman syndrome. *Cell Metab.* **3,** 309–319
11. Yamaguchi, T., Omatsu, N., Morimoto, E., Nakashima, H., Ueno, K., Tanaka, T., Satouchi, K., Hirose, F., and Osumi, T. (2007) CGI-58 facilitates lipolysis on lipid droplets but is not involved in the vesiculation of lipid droplets caused by hormonal stimulation. *J. Lipid Res.* **48,** 1078–1089
12. Miyoshi, H., Perfield, J. W., 2nd, Souza, S. C., Shen, W. J., Zhang, H. H., Stancheva, Z. S., Kraemer, F. B., Obin, M. S., and Greenberg, A. S. (2007) Control of adipose triglyceride lipase action by serine 517 of perilipin A globally regulates protein kinase A-stimulated lipolysis in adipocytes. *J. Biol. Chem.* **282,** 996–1002
13. Shen, W. J., Patel, S., Miyoshi, H., Greenberg, A. S., and Kraemer, F. B. (2009) Functional interaction of hormone-sensitive lipase and perilipin in lipolysis. *J. Lipid Res.* **50,** 2306–2313
14. Granneman, J. G., Moore, H. P., Krishnamoorthy, R., and Rathod, M. (2009) Perilipin controls lipolysis by regulating the interactions of AB-hydrolase containing 5 (Abhd5) and adipose triglyceride lipase (Atgl). *J. Biol. Chem.* **284,** 34538–34544
15. Radner, F. P., Streith, I. E., Schoiswohl, G., Schweiger, M., Kumari, M., Eichmann, T. O., Rechberger, G., Koefeler, H. C., Eder, S., Schauer, S., Theussl, H. C., Preiss-Landl, K., Lass, A., Zimmermann, R., Hoefler, G., Zechner, R., and Haemmerle, G. (2010) Growth retardation, impaired triacylglycerol catabolism, hepatic steatosis, and lethal skin barrier defect in mice lacking comparative gene identification-58 (CGI-58). *J. Biol. Chem.* **285,** 7300–7311
16. Zechner, R., Kienesberger, P. C., Haemmerle, G., Zimmermann, R., and Lass, A. (2009) Adipose triglyceride lipase and the lipolytic catabolism of cellular fat stores. *J. Lipid Res.* **50,** 3–21
17. Bell, M., Wang, H., Chen, H., McLenithan, J. C., Gong, D. W., Yang, R. Z., Yu, D., Fried, S. K., Quon, M. J., Londos, C., and Sztalryd, C. (2008) Consequences of lipid droplet coat protein down-regulation in liver cells. Abnormal lipid droplet metabolism and induction of insulin resistance. *Diabetes* **57,** 2037–2045
18. Chang, B. H., Li, L., Paul, A., Taniguchi, S., Nannegari, V., Heird, W. C., and Chan, L. (2006) Protection against fatty liver but normal adipogenesis in mice lacking adipose differentiation-related protein. *Mol. Cell. Biol.* **26,** 1063–1076
19. Sztalryd, C., Bell, M., Lu, X., Mertz, P., Hickenbottom, S., Chang, B. H., Chan, L., Kimmel, A. R., and Londos, C. (2006) Functional compensation for adipose differentiation-related protein (ADFP) by Tip47 in an ADFP null embryonic cell line. *J. Biol. Chem.* **281,** 34341–34348
20. van der Vusse, G. J., van Bilsen, M., and Glatz, J. F. (2000) Cardiac fatty acid uptake and transport in health and disease. *Cardiovasc. Res.* **45,** 279–293
21. Bachmanov, A. A., Reed, D. R., Beauchamp, G. K., and Tordoff, M. G. (2002) Food intake, water intake, and drinking spout side preference of 28 mouse strains. *Behav. Genet.* **32,** 435–443
22. Bligh, E. G., and Dyer, W. J. (1959) A rapid method of total lipid extraction and purification. *Can. J. Biochem. Physiol.* **37,** 911–917
23. Haemmerle, G., Lass, A., Zimmermann, R., Gorkiewicz, G., Meyer, C., Rozman, J., Heldmaier, G., Maier, R., Theussl, C., Eder, S., Kratky, D., Wagner, E. F., Klingenspor, M., Hoefler, G., and Zechner, R. (2006) Defective lipolysis and altered energy metabolism in mice lacking adipose triglyceride lipase. *Science* **312,** 734–737
24. Nakamura, T. Y., Goda, K., Okamoto, T., Kishi, T., Nakamura, T., and Goshima, K. (1993) Contractile and morphological impairment of cultured fetal mouse myocytes induced by oxygen radicals and oxidants. Correlation with intracellular Ca^{2+} concentration. *Circ. Res.* **73,** 758–770
25. Matsumura, S., Saitou, K., Miyaki, T., Yoneda, T., Mizushige, T., Eguchi, A., Shibakusa, T., Manabe, Y., Tsuzuki, S., Inoue, K., and Fushiki, T. (2008) Mercaptoacetate inhibition of fatty acid β-oxidation attenuates the oral acceptance of fat in BALB/c mice. *Am. J. Physiol. Regul. Integr. Comp. Physiol.* **295,** R82–R91
26. Ohkawa, H., Ohishi, N., and Yagi, K. (1979) Assay for lipid peroxides in animal tissues by thiobarbituric acid reaction. *Anal. Biochem.* **95,** 351–358
27. Suzuki, J., Shen, W. J., Nelson, B. D., Selwood, S. P., Murphy, G. M., Jr., Kanehara, H., Takahashi, S., Oida, K., Miyamori, I., and Kraemer, F. B. (2002) Cardiac gene expression profile and lipid accumulation in response to starvation. *Am. J. Physiol. Endocrinol. Metab.* **283,** E94–E102
28. Granneman, J. G., Moore, H. P., Mottillo, E. P., and Zhu, Z. (2009) Functional interactions between Mldp (LSDP5) and Abhd5 in the control of intracellular lipid accumulation. *J. Biol. Chem.* **284,** 3049–3057
29. Masuda, Y., Itabe, H., Odaki, M., Hama, K., Fujimoto, Y., Mori, M., Sasabe, N., Aoki, J., Arai, H., and Takano, T. (2006) ADRP/adipophilin is degraded through the proteasome-dependent pathway during regression of lipid-storing cells. *J. Lipid Res.* **47,** 87–98
30. Xu, G., Sztalryd, C., Lu, X., Tansey, J. T., Gan, J., Dorward, H., Kimmel, A. R., and Londos, C. (2005) Post-translational regulation of adipose differentiation-related protein by the ubiquitin/proteasome pathway. *J. Biol. Chem.* **280,** 42841–42847
31. Jenkins, C. M., Mancuso, D. J., Yan, W., Sims, H. F., Gibson, B., and Gross, R. W. (2004) Identification, cloning, expression, and purification of three novel human calcium-independent phospholipase A2 family members possessing triacylglycerol lipase and acylglycerol transacylase activities. *J. Biol. Chem.* **279,** 48968–48975
32. Luiken, J. J., van Nieuwenhoven, F. A., America, G., van der Vusse, G. J., and Glatz, J. F. (1997) Uptake and metabolism of palmitate by isolated cardiac myocytes from adult rats. Involvement of sarcolemmal proteins. *J. Lipid Res.* **38,** 745–758
33. Griesel, B. A., Weems, J., Russell, R. A., Abel, E. D., Humphries, K., and Olson, A. L. (2010) Acute inhibition of fatty acid import inhibits GLUT4 transcription in adipose tissue, but not skeletal or cardiac muscle tissue, partly through liver X receptor (LXR) signaling. *Diabetes* **59,** 800–807
34. Balaban, R. S., Nemoto, S., and Finkel, T. (2005) Mitochondria, oxidants, and aging. *Cell* **120,** 483–495
35. Xu, Q., Dalic, A., Fang, L., Kiriazis, H., Ritchie, R. H., Sim, K., Gao, X. M., Drummond, G., Sarwar, M., Zhang, Y. Y., Dart, A. M., and Du, X. J. (2011) Myocardial oxidative stress contributes to transgenic β_2-adrenoceptor activation-induced cardiomyopathy and heart failure. *Br. J. Pharmacol.* **162,** 1012–1028
36. Granneman, J. G., Moore, H. P., Mottillo, E. P., Zhu, Z., and Zhou, L. (2011) Interactions of perilipin-5 (Plin5) with adipose triglyceride lipase. *J. Biol. Chem.* **286,** 5126–5135
37. Wang, H., Bell, M., Sreenevasan, U., Hu, H., Liu, J., Dalen, K., Londos, C., Yamaguchi, T., Rizzo, M. A., Coleman, R., Gong, D., Brasaemle, D., and Sztalryd, C. (2011) Unique regulation of adipose triglyceride lipase (ATGL) by perilipin 5, a lipid droplet-associated protein. *J. Biol. Chem.* **286,** 15707–15715
38. Wang, H., Hu, L., Dalen, K., Dorward, H., Marcinkiewicz, A., Russell, D., Gong, D., Londos, C., Yamaguchi, T., Holm, C., Rizzo, M. A., Brasaemle, D., and Sztalryd, C. (2009) Activation of hormone-sensitive lipase requires two steps, protein phosphorylation and binding, to the PAT-1 domain of lipid droplet coat proteins. *J. Biol. Chem.* **284,** 32116–32125
39. Wang, Z., Heshka, S., Gallagher, D., Boozer, C. N., Kotler, D. P., and Heymsfield, S. B. (2000) Resting energy expenditure-fat-free mass relationship. New insights provided by body composition modeling. *Am. J. Physiol. Endocrinol. Metab.* **279,** E539–E545
40. Gotto, A. M., Jr., Pownall, H. J., and Havel, R. J. (1986) Introduction to the plasma lipoproteins. *Methods Enzymol.* **128,** 3–41
41. Bartholomew, S. R., Bell, E. H., Summerfield, T., Newman, L. C., Miller, E. L., Patterson, B., Niday, Z. P., Ackerman, W. E., 4th, and Tansey, J. T. (2012) Distinct cellular pools of perilipin 5 point to roles in lipid trafficking. *Biochim. Biophys. Acta* **1821,** 268–278
42. Wang, H., Sreenevasan, U., Hu, H., Saladino, A., Polster, B. M., Lund, L. M., Gong, D. W., Stanley, W. C., and Sztalryd, C. (2011) Perilipin 5, a lipid droplet-associated protein, provides physical and metabolic linkage to mitochondria. *J. Lipid Res.* **52,** 2159–2168
43. Stein, O., and Stein, Y. (1968) Structures and physiological roles of 13 integral lipids of bovine heart cytochrome *c* oxidase. *J. Cell Biol.* **36,** 63–77
44. Shinzawa-Itoh, K., Aoyama, H., Muramoto, K., Terada, H., Kurauchi, T., Tadehara, Y., Yamasaki, A., Sugimura, T., Kurono, S., Tsujimoto, K., Mizushima, T., Yamashita, E., Tsukihara, T., and Yoshikawa, S. (2007) Structures and physiological roles of 13 integral lipids of bovine heart cytochrome *c* oxidase. *EMBO J.* **26,** 1713–1725
45. Seddon, M., Looi, Y. H., and Shah, A. M. (2007) Oxidative stress and redox signaling in cardiac hypertrophy and heart failure. *Heart* **93,** 903–907